Supplement of The Cryosphere, 19, 2017–2036, 2025
https://doi.org/10.5194/tc-19-2017-2025-supplement

The Cryosphere Open Access EGU

Supplement of

Evaluation of the Snow Climate Change Initiative (Snow CCI) snow-covered area product within a mountain snow water equivalent reanalysis

Haorui Sun et al.

Correspondence to: Steven A. Margulis (margulis@seas.ucla.edu)

S1. Illustrative fSCA comparison over Tuolumne

Figure S1 provides an illustration of how the Snow CCI and Landsat fSCA differences might lead to the posteriori SWE biases as seen in the ASO verification (Sect. 3.1.2). First, Figure S1a shows how fSCA differs between Snow CCI and Landsat at three points across the 2017 ablation season. In the early ablation season (e.g., April 28th, 2017), Snow CCI fSCA tends to overestimate Landsat fSCA over bare soil areas with fSCA values near 100%, while it underestimates Landsat fSCA over forested areas (Fig. S1c). Forest cover might be expected to moderate the perceived fSCA owing to a combination of the relatively coarse spatial resolution and off-nadir viewing angles observed by MODIS. At off-nadir viewing angles, the coarse spatial resolution of the MODIS sensor may not be able to see through tree gaps, resulting in the forest cover getting smeared out over large footprints. In areas with less forest cover, the MODIS sensor would see the snow cover, but may spatially smear it out, resulting in higher fSCA. The positive biases over bare ground could also result if the observed reflectance over bare soil areas is higher than the value parameterized in the Snow CCI algorithm. Under such conditions, the retrieved fSCA is constrained to 1, which is higher than the corresponding Landsat fSCA. Conversely, during the late ablation season when snow cover depletes (June and July), Snow CCI fSCA is lower than Landsat fSCA across the domain. This is illustrated in Fig. S1b which shows the relationship between fSCA differences and Snow CCI fSCA values on the three sample days. When Snow CCI fSCA is lower than 100%, most differences in fSCA are negative. The correlation is 0.78, indicating that fSCA differences strongly correlate with snow cover extent. The differences change from positive to negative as snow cover depletes. During the warm season, low fSCA values are likely being screened out by the SCAmod algorithm, resulting in an early Snow CCI fSCA snow-free period, as seen in most of the domain in June.

To demonstrate the impact of such fSCA differences on the seasonal evolution of SWE, we choose two snow pillow sites with different forest cover (Fig. S1c): (1) Wilma Lake within a pixel that is moderately forested ($f_{forest} = 14.6\%$) and (2) Tuolumne Meadows within a pixel that is more forested ($f_{forest} = 31.5\%$). At Wilma Lake, the Snow CCI fSCA matches Landsat fSCA well in shaping the curve of posterior fSCA, especially in the late ablation season, leading to a matched SWE time series with a consistent snowmelt season. In contrast, the Snow CCI fSCA is much lower than the Landsat fSCA through the ablation season at the Tuolumne Meadows site. Consequently, Snow CCI posterior SWE is lower and snowmelt is earlier compared to the Landsat posterior SWE. Additionally, the posterior SWE at Wilma Lake is comparable to in-situ SWE measurements, whereas the posterior SWE at Tuolumne Meadows is more negatively biased.

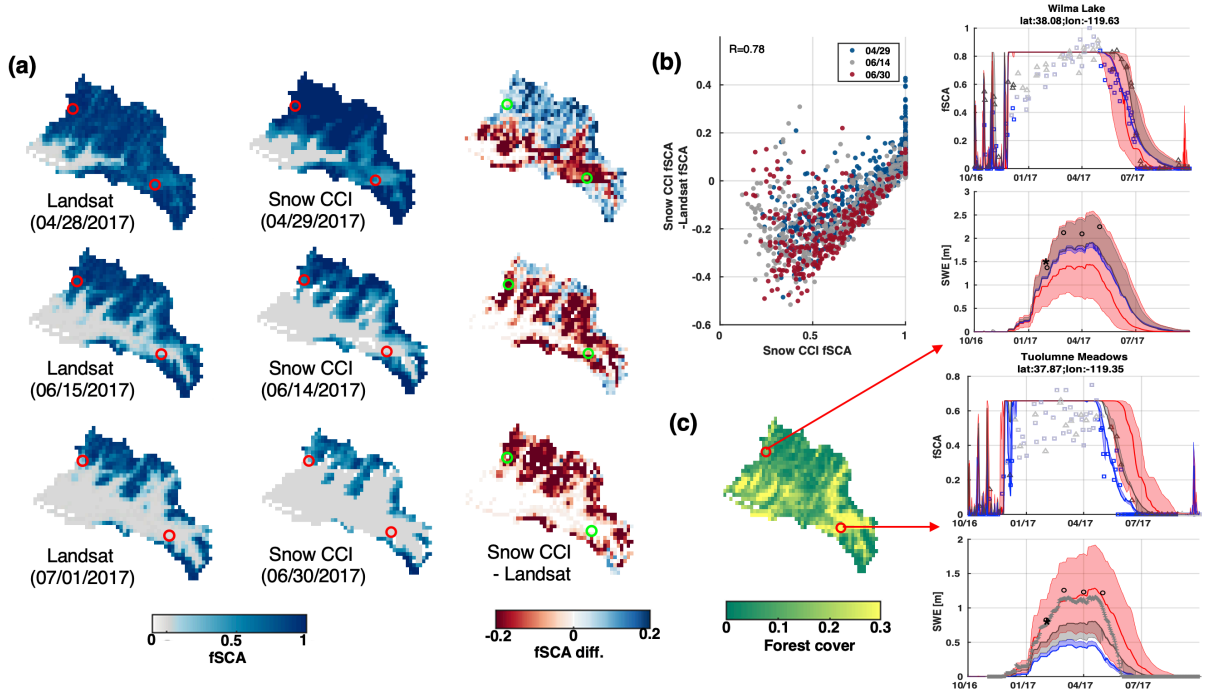

Figure S1. (a) sample assimilated fSCA images (Landsat, near-nadir Snow CCI, and their differences) within the ablation season in WY2017, (b) scatter plot of differences vs. Snow CCI fSCA, and (c) forest cover map and time series of fSCA and SWE before and after data assimilation at two sample sites. The Snow CCI and Landsat fSCA measurements are indicated by the blue squares and grey triangles, respectively. The non-informative fSCA measurements are greyed out. The independent snow pillows, snow courses, and ASO SWE are shown in the grey crosses, black circles, and black asterisk, respectively. The median and inter-quartile range of the ensemble are shown in the solid line and shaded region, respectively. Red curves represent the prior estimates, blue curves represent the Snow CCI posterior estimates, and grey curves represent the Landsat posterior estimates.

S2. Illustrative fSCA and SWE time series at sample in-situ sites in Canadian domains

Figure S2 displays the typical fSCA and SWE time series at sample in-situ sites in Bow and Lajoie. We choose three in-situ sites with varying forest and snow cover conditions: (1) Mount Odlum within a pixel that is densely forested ($f_{forest} = 53\%$), (2) Sunshine Village within a pixel that is moderately forested ($f_{forest} = 29\%$), and (3) Downton Lake within a pixel that is closest to bare soil ($f_{forest} = 12\%$). Locations of these sites are indicated in Fig. 1. Specific years are chosen because (1) the number of Snow CCI fSCA is sufficient that can well constrain the prior estimates of fSCA and (2) snow pillow SWE measurements are representative that can match the reanalysis estimates.

In the Mount Odlum example (WY2010), Snow CCI fSCA is generally lower than Landsat fSCA, leading to an earlier snowmelt and lower SWE compared to both the Landsat reanalysis estimates and snow pillow measurements. The prior

estimates of SWE and fSCA have large uncertainties due to difficulties in parameterizations over forested areas. The posterior Snow CCI fSCA is sensitive to the low fSCA values in the early ablation season at the expense of high fSCA values later (late June-early July).

At Sunshine Village (WY 2006), posterior SWE estimates from Snow CCI reanalysis are more accurate than the Landsat reanalysis when compared to snow pillow and snow courses measurements. The SWE evolution curve and peak SWE values from Snow CCI estimates closely match the in-situ measurements across the WY, whereas the Landsat estimates are essentially the same as prior estimates due to the limited number of assimilated fSCA.

At Downton Lake (WY 2016), Snow CCI fSCA is saturated (equal to 1) during the snow accumulation season and is higher than Landsat fSCA, resulting in higher SWE and a later snowmelt season. It is likely that the observed reflectance is higher than the model limit and the retrieved Snow CCI fSCA is constrained to 1 during the accumulation season.

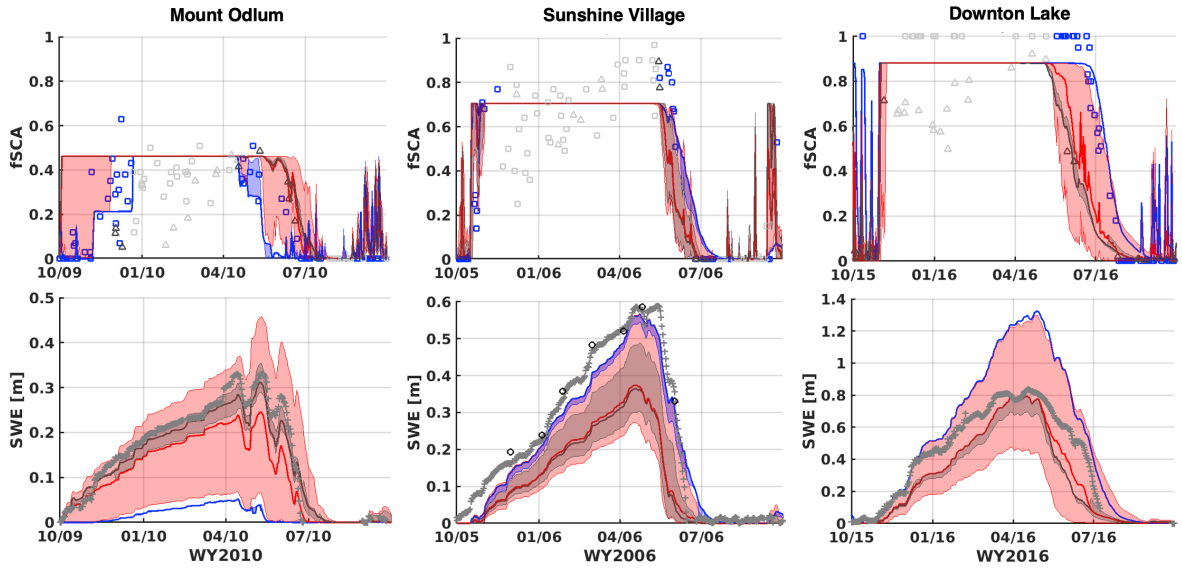

Figure S2. Time series of fSCA and SWE before and after data assimilation at three in-situ sites in Bow and Lajoie domains (red curves represent the prior estimates, blue curves represent the Snow CCI posterior estimates, and grey curves represent the Landsat posterior estimates). The median and inter-quartile range of the ensemble are shown in the solid line and shaded region, respectively. The Snow CCI and Landsat fSCA measurements are indicated by the blue squares and grey triangles, respectively. The independent snow pillows and snow courses SWE are shown in the grey crosses and black circles, respectively.

S3. ASO SWE comparison over Tuolumne

Statistics from the comparison of reanalysis prior and posterior SWE for both Landsat and Snow CCI to all available ASO days over Water Years 2015-2018 are shown in Table S1.

Table S1. SWE comparison statistics between ASO SWE estimates against prior and posterior snow reanalysis SWE on ASO measurement days (Day of Water Year, DOWY).

ASO basin	Water Year	Day of Water Year	Correlation			RMSD (m)		
			prior	Landsat posterior	Snow CCI posterior	Prior	Landsat posterior	Snow CCI posterior
Tuolumne	2015	140	0.58	0.82	0.7	0.07	0.1	0.1
		156	0.61	0.86	0.76	0.09	0.09	0.1
		176	0.53	0.86	0.78	0.08	0.06	0.07
		185	0.48	0.83	0.75	0.08	0.05	0.06
		191	0.45	0.81	0.72	0.12	0.07	0.09
		197	0.45	0.82	0.73	0.11	0.06	0.08
		209	0.44	0.79	0.7	0.11	0.07	0.09
		213	0.47	0.79	0.7	0.07	0.04	0.05
		240	0.62	0.81	0.66	0.07	0.05	0.06
		251	0.7	0.72	0.52	0.03	0.03	0.03
	2016	178	0.66	0.9	0.84	0.41	0.26	0.37
		183	0.64	0.89	0.85	0.37	0.22	0.32
		190	0.62	0.9	0.84	0.36	0.21	0.32
		199	0.65	0.91	0.85	0.34	0.18	0.28
		209	0.68	0.92	0.83	0.39	0.24	0.34
		222	0.69	0.93	0.86	0.36	0.19	0.29
		240	0.56	0.89	0.87	0.28	0.15	0.19
		282	0.77	0.82	0.6	0.04	0.03	0.04
	2017	154	0.59	0.88	0.8	0.45	0.3	0.48
		183	0.54	0.92	0.87	0.6	0.27	0.46
		214	0.6	0.91	0.85	0.58	0.29	0.5
		282	0.31	0.82	0.72	0.28	0.17	0.2
	2018	205	0.59	0.86	0.79	0.3	0.19	0.4
		240	0.51	0.82	0.73	0.17	0.11	0.35